Accepted Manuscript

Highly selective on-off fluorescence recognition of Fe3+ based on a coumarin derivative and its application in live-cell imaging

Sona Warrier, Prashant S. Kharkar

PII:	S1386-1425(17)30628-5
DOI:	doi: 10.1016/j.saa.2017.07.068
Reference:	SAA 15355
To appear in:	*Spectrochimica Acta Part A: Molecular and Biomolecular Spectroscopy*
Received date:	24 April 2017
Revised date:	15 July 2017
Accepted date:	30 July 2017

Please cite this article as: Sona Warrier, Prashant S. Kharkar , Highly selective on-off fluorescence recognition of Fe3+ based on a coumarin derivative and its application in live-cell imaging, *Spectrochimica Acta Part A: Molecular and Biomolecular Spectroscopy* (2017), doi: 10.1016/j.saa.2017.07.068

Highly selective on-off fluorescence recognition of Fe^{3+} based on a coumarin derivative and its application in live-cell imaging

Sona Warrier and Prashant S. Kharkar*

Department of Pharmaceutical Chemistry, Shobhaben Pratapbhai Patel School of Pharmacy and Technology Management, SVKM's NMIMS,

V. L. Mehta Road, Vile Parle (West), Mumbai-400 056. India.

Abstract

A novel coumarin chemosensor, 7-hydroxy-2-oxo-N-(pyridin-2-ylmethyl)chromene-3-carboxamide **(Probe 1)**, demonstrated significant selectivity towards Fe^{3+} ions. **Probe 1** exhibited high fluorescence emission profile at 447 nm, excellent selectivity towards Fe^{3+} over other biologically important metal ions (Al^{3+}, Ba^{2+}, Co^{2+}, Cu^{2+}, Zn^{2+}, Cd^{2+}, Hg^{2+}, Pb^{2+} and Sn^{2+}). Interestingly, there was ~30-fold decrease in fluorescence intensity upon Fe^{3+} binding. The limit of detection of Fe^{3+} was found to be 0.76 μM (~ 40 ppb). **Probe 1** also exhibited high potential as an intracellular chemosensor for Fe^{3+}.

Keywords

Coumarin, fluorescent chemosensor, fluorescence quenching, Fe^{3+} probes, live-cell imaging

1. Introduction

The role of iron as a micronutrient in cellular functions is crucial for various life processes. Iron is essential for cellular metabolism as it forms a part of the structure of many enzymes and proteins [1]. Iron is distributed in hemochrome which consists of > 50% of total iron in the body. Nevertheless, up-regulation (hyperferremia) or down-regulation (hypoferremia) of iron concentrations in the body gives rise to disease conditions related to iron trafficking and storage [2]. High concentrations of iron cause nausea, abdominal pain, gastric problems and hyperferremic and hypotransferrinemic disorders. Likewise, its deficiency causes anaemia and related discrepancies such as impaired cognitive function, lethargy, low immunity, etc. When blood comes in contact with atmospheric air, Fe^{2+} gets oxidised to Fe^{3+} that causes a colour change from red to brown. Although iron is absorbed and largely used in its iron (II) oxidation state, it is stored in ferritin as the iron (III) state. Homeostasis of iron is a significant aspect in neuro-inflammation and progression of Alzheimer's disease [3-5]. Although the human body can

balance iron concentrations to some extent, it is important to utilize analytical techniques for sensitive detection of iron for biomedical purposes [6].

Various techniques are available for the detection of metal ions, which include atomic absorption spectroscopy (AAS), voltammetry, colorimetry and electrochemical methods. The downside of such techniques is that they require sophisticated equipments, tedious sample preparation and specialized skills [7-8]. A recent advancement in analytical technology is the field of chemosensors. These are fluorescent molecules which exhibit changes in their photophysical properties in presence of a desired analyte. Their popularity can be attributed to advantages such as sensitivity, selectivity, non-destructiveness, ease of handling and rapid visual detection [9-11]. Such chemosensors can be designed by systematic optimization of their electronic structure by modification/addition of functional groups to achieve desired properties, which in turn are favourable for the detection of trace levels of metal ions in biological fluids [12].

The present work utilizes coumarins as chemosensors due to their excellent spectroscopic properties, light stability and less toxicity [13]. The design of the probe is based on fluorescence switching mechanism wherein the photophysical property of the molecule is altered upon interaction with the desired analyte [14-16]. According to the concept of hard-soft acid-base theory, probes attached to the recognition moiety with N and O atoms can display good affinity towards Fe^{3+} [17]. Reflecting on these ideas, a novel chemosensor (**Probe 1**) was synthesized by a facile method that detects Fe^{3+} by fluorescence quenching mechanism (**Scheme 1**). This molecule offers several advantages such as ease of synthesis, highly sensitive detection, good aqueous solubility, stability and cell-staining behaviour.

2. Experimental

2.1. General

Unless stated, all reagents and solvents are of analytical grade and used without further purification. Nuclear magnetic resonance (NMR) spectra were obtained on Brucker NMR 300 instrument, and chemical shifts were given in ppm from tetramethylsilane (TMS) as internal standard. Mass spectra (MS) were recorded on a Shimadzu 8040 LC-MS/MS system. Fluorescence emission spectra were conducted on a JASCO FP-8000 Series fluorescence spectrofluorometer. UV-Vis spectra were obtained on a Perkin Elmer Lambda 25 UV-Vis spectrometer.

2.2. Synthesis

The synthetic route for **Probe 1** is shown in Scheme 1.Ethyl 7-hydroxy-2-oxochromene-3-carboxylate **(1)** was prepared from 2,4-dihydroxybenzaldehyde according to literature method [18]. Compound **1** was further hydrolysed using 0.5 M NaOH to give 7-hydroxy-2-oxochromene-3-carboxylic acid **(2)** which was further coupled with 2-picolylamine to obtain **Probe 1**.

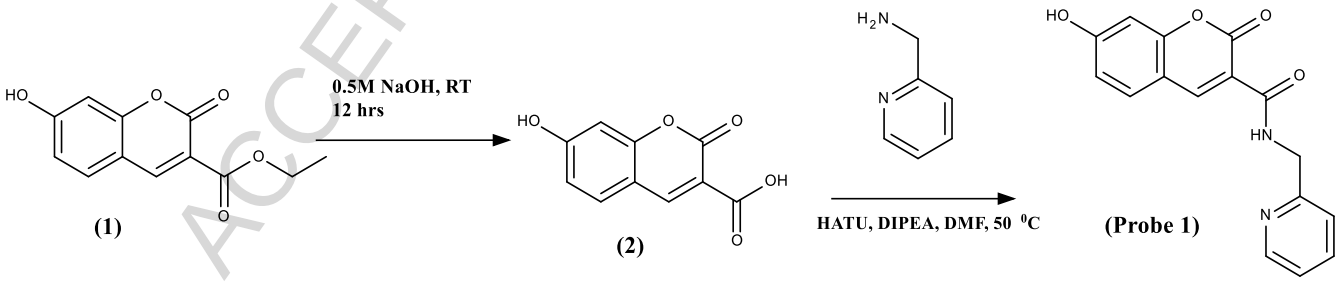

Scheme 1. Synthesis of **Probe 1**

Synthesis of 7-hydroxy-2-oxo-N-(pyridin-2-ylmethyl) chromene-3- carboxamide (Probe 1).

To a stirred solution of 2-picolylamine (280 mg, 2.59 mmol) and **2** (750 mg, 3.88 mmol) in anhydrous DMF (4 mL), DIEA (2.2 mL, 12.91 mmol) was added slowly. With stirring, HATU (1.6 g, 5.0 mmol) was added and the reaction was warmed to 50°C and stirred further for 3 h.

The reaction mixture was then diluted with water and extracted with EtOAc (3x20 mL). The combined organic layers were dried with anhydrous $NaSO_4$ and concentrated in vacuo to yield the crude product which was purified by column chromatography using EtOAc : pet ether (7:3) as eluent to obtain **Probe 1** as yellow solid (820 mg, 76%).^{1}H NMR (400MHz, DMSO-*d6*) (δppm): 4.65 (d, 2H, -NH-C$\underline{H}_2$), 6.9 (dd, 2H, coumarin-H), 7.3 (m, 2H, coumarin-$\underline{H}$, Pyr-$\underline{H}$), 7.7 (m, 2H, coumarin-$\underline{H}$, Pyr-$\underline{H}$), 8.55 (d, 1H, Pyr-$\underline{H}$), 8.8 (s, 1H, -O$\underline{H}$), 9.4 (t, 1H, Pyr-$\underline{H}$), 11.08(s, 1H, -N$\underline{H}$-); LC-MS (ESI): 297 $[M+H]^+$.

2.3. UV–Vis and fluorescence spectral measurements

Aqueous stock solutions (10 mM) of the appropriate metal salts were prepared. Stock solution of **Probe 1** (1 mM) was prepared in DMSO. Further, working standards were freshly prepared. For all fluorescence measurements, excitation was set at 385 nm with excitation and emission slit widths set at 5.0 nm. UV/Vis and fluorescence titration experiments were performed using 10 μM and 1 μM of **Probe 1**, respectively, in water with varying concentrations of the metal salts. The metal salts used were $AlCl_3$, $BaCl_2$, $CuCl_2.2H_2O$, $CoCl_2.6H_2O$, $CdCl_2$, $FeCl_3$, $HgCl_2$, $PbCl_2$, $MgCl_2$, $ZnCl_2$, and $SnCl_2.2H_2O$.

2.4. Fluorescence titration involving Fe^{3+}

The titration experiments were performed at **Probe 1** concentration 1 μM and Fe^{3+}concentrations at 0.0, 0.2, 0.4, 0.5, 0.8, 1, 2, 4, 5, 10 μM. Fluorescence spectra were recorded at RT.

2.5. Solubility and effect on pH

Direct kinetic solubility was performed with **Probe 1** using standard procedures [19] to confirm the aqueous solubility of the probe as well as to explore its behaviour in different pH solutions.

2.6. Effect of solvents

The fluorescence behaviour of **Probe 1** in the presence of different solvents with varying polarity was investigated. 1 µM solution of the **Probe 1** was prepared in MeOH, EtOAc, EtOH, DMF and DMSO and their fluorescence spectra were recorded.

2.7. Cell imaging

LLC-MK2 cell lines were used for fluorescence imaging. Cell lines were cultured in Dulbecco's Modified Eagle's medium (Gibco BRL, USA), supplemented with 10% (v/v) heat-inactivated fetal calf serum (FCS) (cell Clone), 100 μg/mL penicillin,100 μg/mL streptomycin, and 0.25 mM L-glutamine, at 37 °C in 5% CO_2 humidified air. As soon as the cells reached confluency, cell density was adjusted to 1.0×10^5 cells/well in culture media. To determine the cell permeability of Fe^{3+}, the cells were incubated with **Probe 1** (1µM) for 30 mins at 37 °C. Upon addition of 10 equivalents of Fe^{3+} onto the cells, the images were observed under phase-contrast microscope with DAPI filter.

2.8. MTT Assay

LLC-MK2 cell in the concentration of 5×10^4 cells/mL were seeded into a 96-well, microplate (Nunc, DNK). 100µL of complete medium was added to all wells and plates were incubated in 5% CO_2 and 37 °C. After 24 hours, the cells were treated with **Probe 1** (1, 10, 50, 100, 200 µM) then incubated under 5% CO_2 at 37 °C. Post-24 hrs, cells were washed with DPBS followed by addition of MTT [3-(4,5-dimethylthiazol-2-yl)-2,5-diphenyltetrazolium bromide] solution (5mg/mL, Sigma) and again incubated under 5% CO_2 at 37 °C for 4 hrs. The MTT solution was removed and 150 μL of DMSO was added to dissolve the crystals and incubated for 10 mins. The optimal density (OD) value was measured by a microplate reader (Epoch 2 Biotek) at 570

nm. The cell viability was calculated as (mean OD in treated wells/mean OD in control wells) × 100.

3. Results and Discussion

3.1. UV–Vis spectral measurements

When 10 equivalents of various metal ions (Al^{3+}, Ba^{2+}, Co^{2+}, Cu^{2+}, Zn^{2+}, Cd^{2+}, Hg^{2+}, Fe^{3+}, Pb^{2+} and Sn^{2+}) were added to **Probe 1** (10 μM), only Cu^{2+}, $Co^{2+}$and Fe^{3+} produced an instant color change (colourless to light yellow). The interaction of **Probe 1** with various metal ions was initially studied by UV–Vis spectroscopy (Figure 1). The absorbance of **Probe 1** decreased significantly, compared to other metal ions in the presence of Fe^{3+} ions. It was observed that the interaction between **Probe 1** and Fe^{3+} was very fast and efficient.

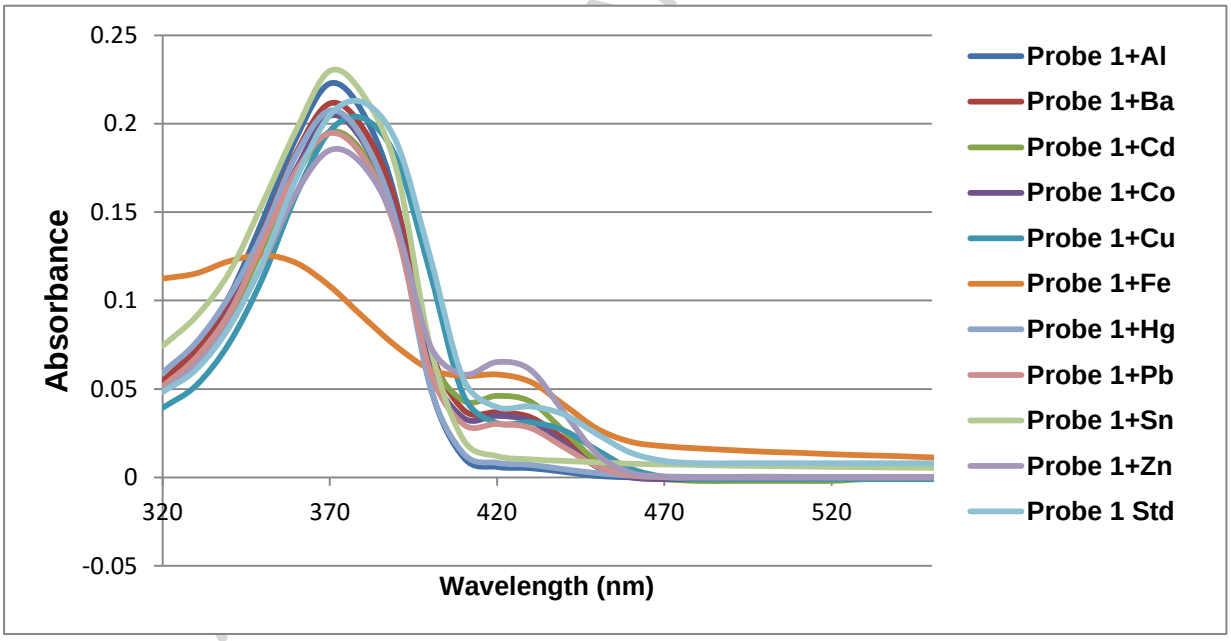

Figure 1. UV–Vis absorption spectra of **Probe 1** (10 μM) upon addition of respective metal ions (100 μM) in water.

3.2. Fluorescence spectral measurements

Furthermore, the photophysical properties of **Probe 1** in the presence of a wide range of environmentally and physiologically significant metal ions such as Al^{3+}, Zn^{2+}, Cu^{2+}, Ba^{2+}, Co^{2+}, Sn^{2+}, Cd^{2+}, $Pb^{2+}$and Hg^{2+} as well as Fe^{3+} were investigated. **Probe 1** (1μM) showed a significant emission upon excitation at 385 nm (Figure 2a). There was no obvious spectral change in the intensity of **Probe 1** when other cations were added. However, major quenching of fluorescence intensity occurred with Fe^{3+} ions. There was slight quenching observed with Al^{3+}, Sn^{2+} and Hg^{2+} while other cations revealed almost insignificant response (Figure 2b). Thus, it can be established that the selectivity of **Probe 1** for Fe^{3+} ions over other cations, in aqueous media, is remarkably high.

a)

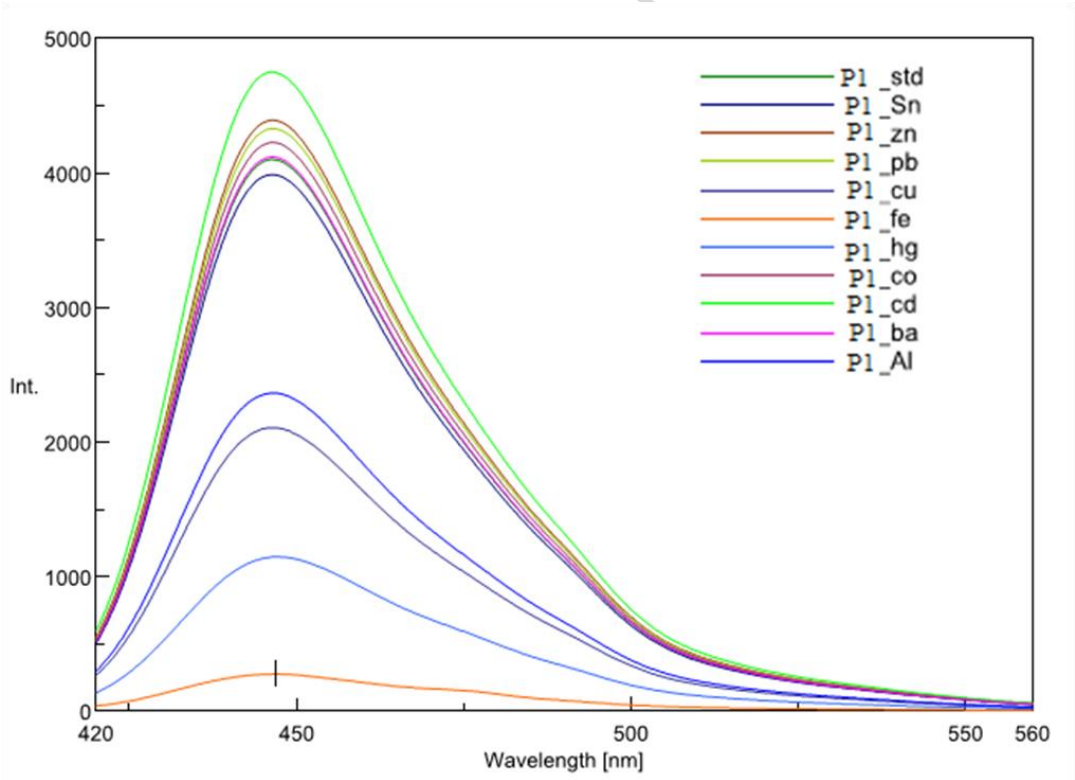

b)

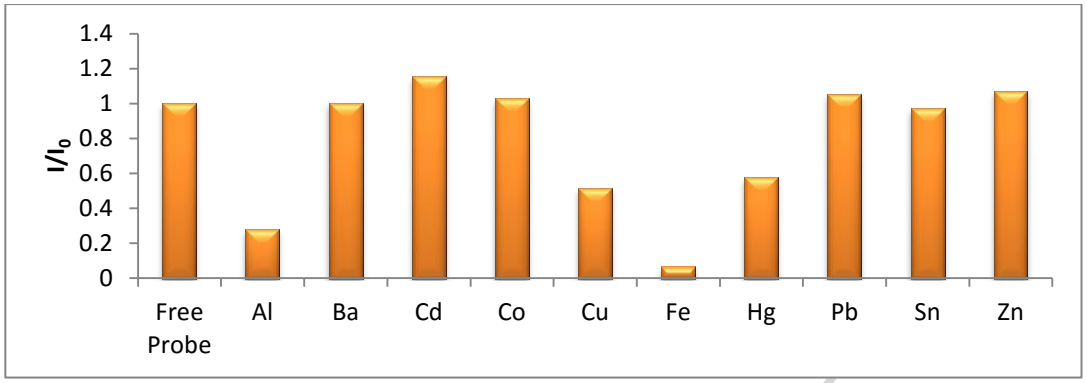

Figure 2. a) Fluorescence spectra of **Probe 1** (1 μM) upon addition of metal salts (10 equiv.) Al^{3+}, Ba^{2+}, Co^{2+}, Cu^{2+}, Zn^{2+}, Cd^{2+}, Hg^{2+}, Fe^{3+}, Pb^{2+} and Sn^{2+} at λ_{ex} of 385 nm, b) relative responses at 447 nm (λ_{em}) of **Probe 1** upon addition of various metal ions upon excitation at 385 nm.

To further validate the utility of **Probe 1,** fluorescence titration experiment was carried out in the presence and absence of Fe^{3+} by mixing **Probe 1** (1μM) with increasing concentrations of Fe^{3+} (0.2, 0.4, 0.5, 0.8, 1, 2, 4, 5, 10 equivalents) (Figure 3).The signals were measured within one minute of addition of Fe^{3+} ions. As Fe^{3+} concentration increased, the high fluorescence intensity of **Probe 1** at 447 nm decreased almost 30-fold when excited at 385 nm (λ_{ex}). The fluorescence quenching occurred in a linear fashion as the concentration of the analyte increased.

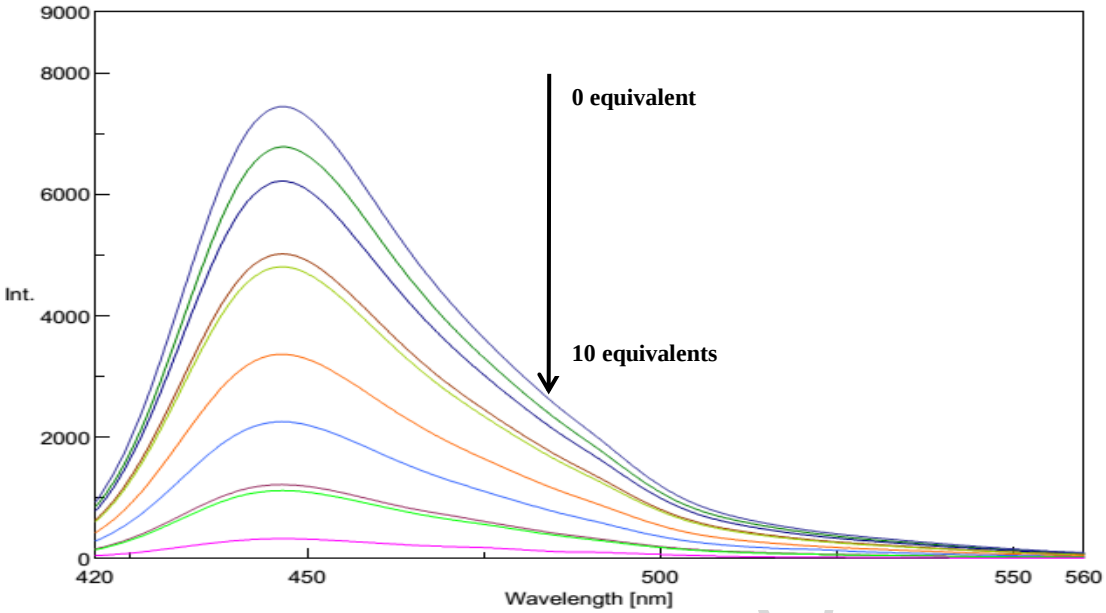

Figure 3. Fluorescence titration spectra of **Probe 1** (1 μM, λ_{ex}= 385 nm) upon addition of increasing concentrations of Fe^{3+} ions metal chloride (0, 0.2, 0.4, 0.5, 0.8, 1, 2, 4, 5, 10 μM) at room temperature.

3.3. Determination of detection limit

To analyse the quenching process of the fluorophore-metal system, Stern-Volmer equation (Equation 1) was used for determining the type of quenching. Linear plot of Stern-Volmer establishes that the quenching is a static type of quenching and not dynamic quenching [20,21].

$I_0/I = 1 + K_{SV}[Q]$ ..... (1)

where I_0 and I are the fluorescence intensities at 447 nm in the absence and presence of Fe^{3+} ions, respectively. K_{SV} is the Stern–Volmer fluorescence quenching constant, which is related to the quenching efficiency of the quencher, and [Q] is the concentration of the quencher, [Fe^{3+}].

In the presence of different concentrations of the quencher, fluorescence intensity was reduced from I_0 to I. The fluorescence data were then analysed by plotting a graph of I_0/I versus [Fe^{3+}]. The Stern–Volmer plot of I_0/I versus [Q] (Figure 4) showed a linear relationship between the

fluorescence response and [Fe^{3+}] in the range of $0.2x10^{-6}$ M to $10x10^{-6}$M with a correlation coefficient of 0.995. The linear Stern–Volmer plot indicated that the quenching was static for **Probe 1-Fe^{3+}** system. From the linearity graph, the limit of detection (LOD) for Fe^{3+} was calculated to be 0.76 μM, which is much lower than WHO (World Health Organization) guidelines (5 μM) for Fe^{3+} ions in drinking water.[2]

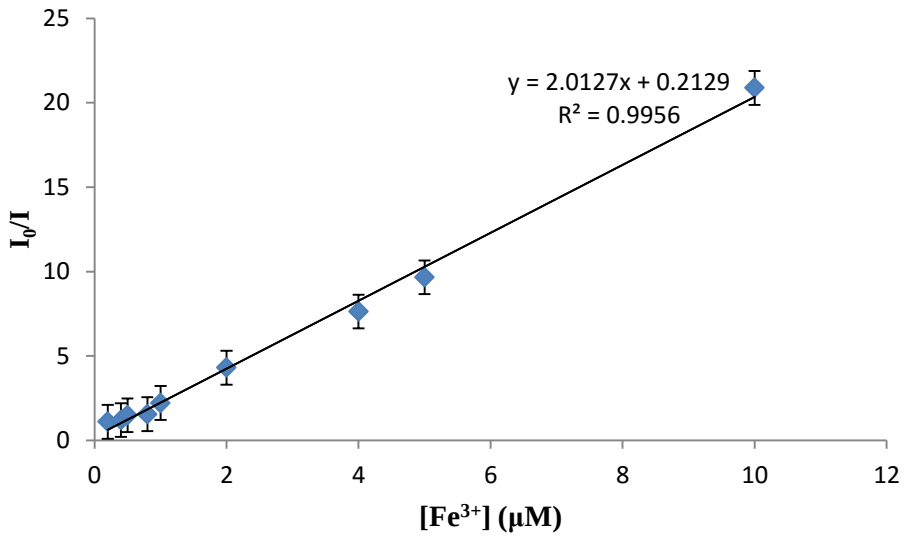

Figure 4. Emission (at 447 nm) of **Probe 1** (1 μM) at different concentrations of Fe^{3+} (0.2, 0.4, 0.5, 0.8, 1, 2, 4, 5, 10 μM) are normalized between the minimum (0.0 μM Fe^{3+}) and the maximum emission intensities.

3.4.Selectivity of Probe 1

The interference of other metal cations that could possibly coexist with Fe^{3+} was explored by carrying out competition experiments. To utilize **Probe 1** as a selective sensor for Fe^{3+} ions, the fluorescence responses of **Probe 1** was investigated in the presence of co-existing metal ions such as Al^{3+}, Ba^{2+}, Cd^{2+}, Cu^{2+}, Co^{2+}, Hg^{2+}, Pb^{2+}, Sn^{2+}, Zn^{2+}, Na^{+}, K^{+}, Mg^{2+}, Mn^{2+}, Ca^{2+}. As shown in Figure 5, the presence of other metal ions did not interfere the quenching of **Probe 1**

by Fe^{3+} and the intensity changes due to Fe^{3+} were not affected by the addition of co-existing metal ions. The results show that **Probe 1** was a selective On-Off sensor for Fe^{3+}.

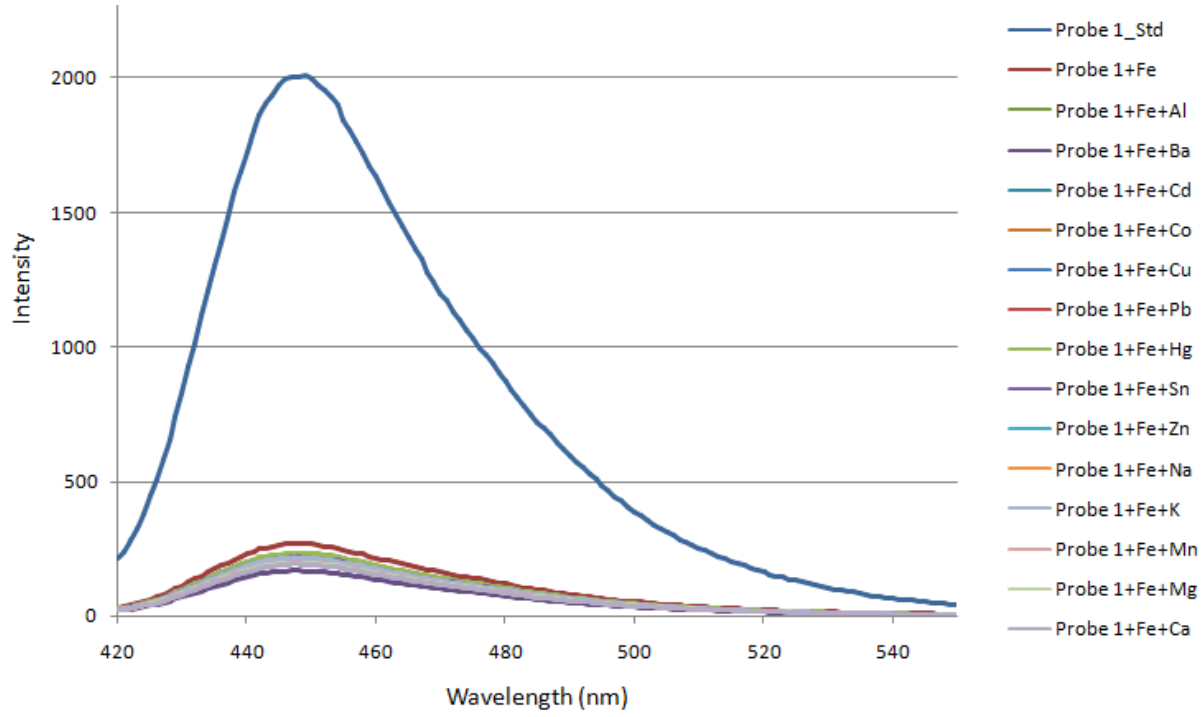

Figure 5. Fluorescence emission responses of **Probe 1** containing Fe^{3+} and other co-existing metal ions; λ_{ex}= 385 nm.

3.5. Ratiometric measurements of Probe 1 in the presence of Fe^{3+} ions

Since there is no shift in the emission wavelength of **Probe 1** upon addition of Fe^{3+} ions, ratiometric measurements were carried out by employing another fluorescent probe having a different λ_{max} and that has Fe^{3+} chelating properties. 8-hydroxyquinoline (8-HQ) is extensively used in iron chelation therapy and has affinity towards Fe^{3+} ions. Therefore, 8-hydroxyquinoline was employed for ratiometric calculations (λ_{max}= 255 nm). The UV-Vis absorbances of **Probe 1** (λ_{max}=385 nm) and 8-HQ (λ_{max}= 255 nm) were measured in the presence of Fe^{3+} ions. Upon the addition of increasing amounts of Fe^{3+}, the absorbance ratio at 385 nm and 255 nm (A_{385} nm/ A_{255} nm) also decreased linearly with the concentration of Fe^{3+} (0-10 equiv) (Figure 6). These

ratiometric measurements were performed to allow correction of subtle variations independent of the sample conditions (e.g. concentration of the probe, sample thickness, intensity of illumination).

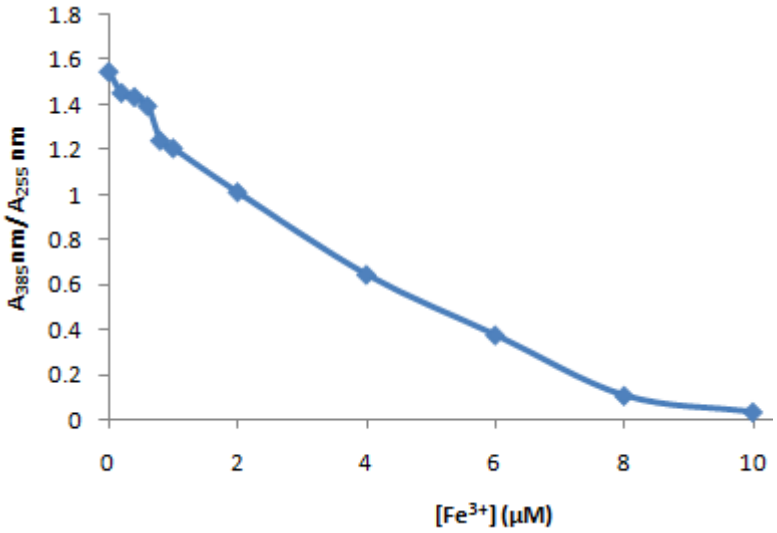

Figure 6. Ratiometric calibration curve A_{385nm}/ A_{255nm} as a function of Fe^{3+} concentration.

3.6.Aqueous solubility and the effect of pH

Aqueous solubility and stability forms an integral part in the discovery of fluorescent probes since it has a great influence on assays involving biological systems such as cells. The solubility of **Probe 1** was explored by direct "kinetic" solubility conditions. The probe was also subjected to different pH conditions for 2 days. The probe was found to have a aqueous solubility of more than 10 µM and that it was stable over a range of pH (1-8).

3.7. Effect of solvents

To get a view of the practical application potential, particularly in material sciences, we examined the fluorescence intensity of **Probe 1** in different solvents. Since, in many cases, the influence of solvents is significant for the fluorescence spectra of complexes, fluorescence emissions of **Probe 1** (1µM) in different solvents were explored (Figure 5) [22-25]. There was

no significant change in the fluorescence intensity of **Probe 1** in different solvents like MeOH, EtOH, EtOAc, DMF and DMSO. Thus, it can be deduced that **Probe 1** can be employed with a variety of solvents without significant changes in its photophysical properties.

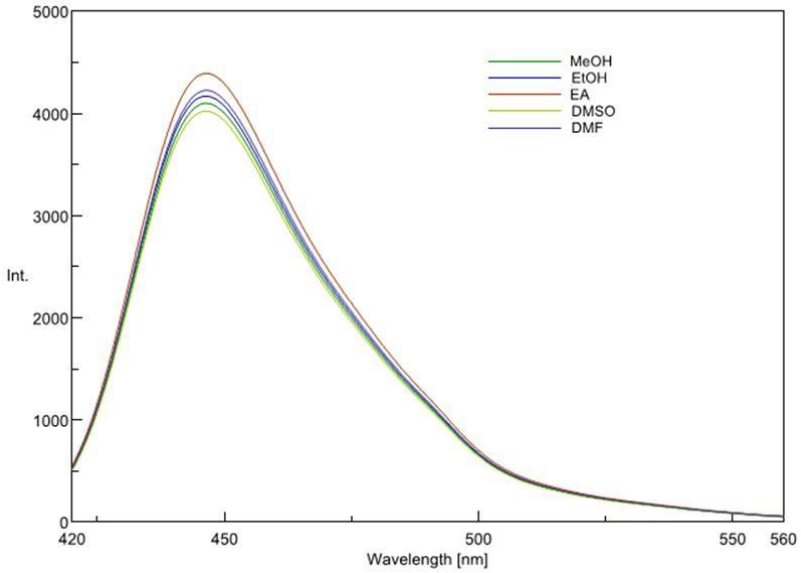

Figure 7. Fluorescence emission spectra of **Probe 1** (1μM) in different solvents.

3.8. Mechanism of fluorescence quenching

The presence of a 7-OH group and 3-CONH- group in **Probe 1** make it highly fluorescent due to the transfer of electrons within the molecule, like a push-pull system. Therefore, when chelation occurs, there is a transfer of charges within the **Probe 1**-metal system which in turn causes a decrease in the fluorescence intensity of the molecule [26,27]. Consequently, it would be rational to infer that the mechanism of fluorescence quenching of **Probe 1** in the presence Fe^{3+} could be attributed to ligand-metal charge transfer (LMCT) mechanism. There occurs a charge transfer which is initiated by the binding of Fe^{3+} ions to **Probe 1**. This hypothesis is supported by the fact that Fe^{3+} is known to be paramagnetic with an unfilled *d* shell that would take part in the energy and/or electron transfer processes leading to quenching of the fluorescence [28-30]. When Fe^{3+} comes in contact with **Probe 1**, the fluorophore opens a nonradiative deactivation channel

induced by unfilled *d* shell and paramagnetism, to cause electron transfer that is, resulting in quenching of fluorescence. The interaction between **Probe 1** and Fe^{3+}could occur at C=O, –NH and the nitrogen in pyridine ring which could be identified as binding to transition and post-transition metals [31,32]. Hence, the mechanism of LMCT could occur rapidly due to strong paramagnetic quenching property of Fe^{3+} that covers all other mechanisms for fluorescence quenching.

3.9. Cell imaging and MTT assay

Further, the practical application of **Probe 1** was explored as an intracellular chemosensor for Fe^{3+} (Figure 6). The imaging of cells by **Probe 1** was assessed by phase-contrast microscopy with DAPI fluorescence filter. As seen from the bright-field image, LLC-MK2 cells incubated with 1 μM of **Probe 1** for 30 min at 37 °C show cell viability (Figure 6a) with strong intracellular background fluorescence (Figure 6b). The cells that were pre-incubated with **Probe 1** were supplemented with 10 μM of Fe^{3+} for 10 min at 37 °C that reduced the intracellular background fluorescence (Figure 6c). These results demonstrated the potential utility of **Probe 1** as cell- permeable, chemosensor of Fe^{3+} in living cells.

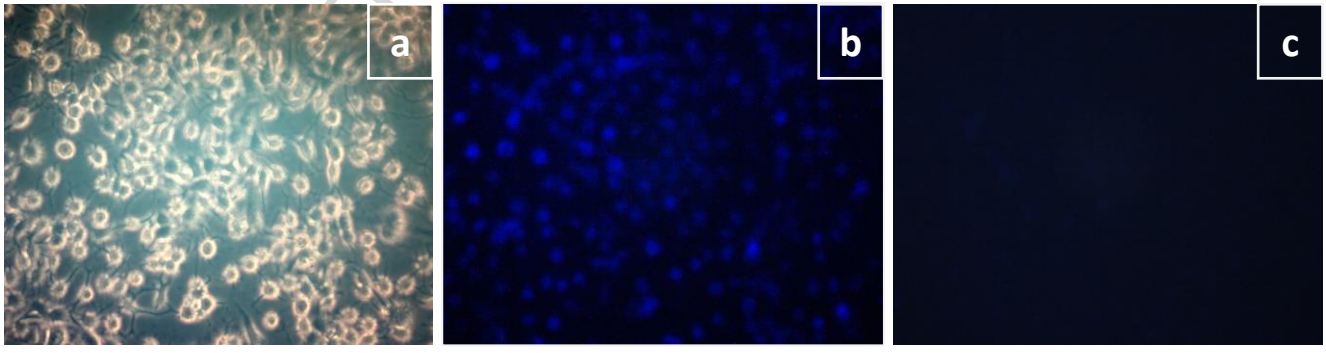

Figure 8. Live-cell imaging of intracellular Fe^{3+}: (a) Bright field transmission image of LLC-MK2 cells incubated with 1 μM of **Probe 1** (b) Fluorescence image of LLC-MK2 cells supplemented with 1 μM of **Probe 1** in the growth media for 30 min at 37°C (c) LLC-MK2 cells

incubated with 1 μM of **Probe 1** in the growth media for 30 min at 37°C and then further incubated with 10 μM $FeCl_3$ for 10 min at 37°C.

Consecutively, the toxicity evaluation of **Probe 1** was carried out by MTT assay that exhibited dose-dependent decrease in cell viability. There was no significant loss of viable cells at lower concentrations indicating relatively non-toxic nature of **Probe 1**. This observation supports potential utility of **Probe 1** for cell biology applications (Figure 7).

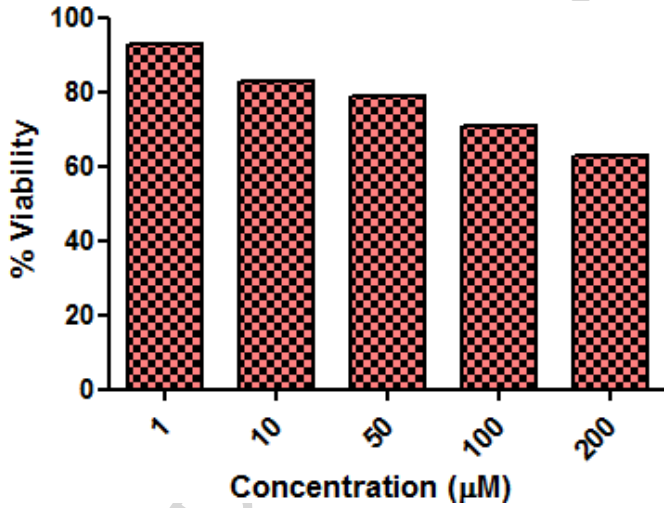

Figure 9. Cytotoxicity of **Probe 1** on LLC-MK2 cells. Cell viability was assayed by the MTT method (values: mean ± s.d.)

3.10. Performance comparison

The analytical performance of the probe proposed in the present work towards Fe^{3+} was compared with other reported fluorescent probes based on various fluorophore derivatives as shown in Table S1 (ESI). Although it can be seen that most of these probes have good selectivity towards Fe^{3+}, some have dual-sensing mechanisms that involves Fe^{2+} and Cu^{2+} that would make them less selective towards Fe^{3+}, in the presence of Cu^{2+} [21,34,38]. The fluorescent probe developed in this work exhibits selectivity only towards Fe^{3+} and has no interference from other transition metals. Some of the fluorescent probes listed in the table do not mention their

detection limits [7,20,37], while some probes have higher detection limits than the probe presented in this work [21,36]. Therefore, overcoming the disadvantages of expensive starting materials [20], lower yields and narrow linear range, this small molecule fluorescent probe aims to provide a valuable sensor for further biomedical applications.

4. Conclusion

In conclusion, a novel coumarin chemosensor was synthesized by a simplistic method using inexpensive starting materials and evaluated for its sensing abilities towards Fe^{3+} ions. **Probe 1** demonstrated highly selective fluorescence turn-off response only in the presence of Fe^{3+}. LMCT mechanism is known to facilitate the quenching processes by the fluorophore. **Probe 1** shows no interference from other metal ions. The limit of detection for **Probe 1** was found to be 0.76 μM. **Probe 1** can also be utilized in studying the cellular functions involving Fe^{3+} in various disease and pathological conditions.

Conflict of Interest

The authors confirm that this article content has no conflict of interest.

Acknowledgements

Ms. Sona would like to acknowledge SVKM's NMIMS for PhD fellowship during the course of this work. The authors acknowledge the help and valuable assistance of Dr. Nishigandha Naik and Ms. Amruta Naik from *Haffkine Institute for Training, Research and Testing***,**Parel, Mumbai for providing facility for fluorescence spectrophotometer.

References

1. C. Han, R. Wang, K. Wang, H. Xu, M. Sui, J. Li, K. Xu, Biosens. Bioelectron. 83 (2016) 229-236.

2. S. Bishnoi, M.D. Milton, J. Photochem. Photobiol. A: Chem. 335 (2017) 52-58.

3. S.K. Sahoo, D. Sharma, R.K. Bera, G. Crisponi, J.F. Callan, Chem. Soc. Rev. 41(2012) 7195-7227.

4. R.H. Crabtree, Science. 266 (1994) 1591- 1593.

5. J.R. Burdo, J.R. Connor, BioMetals. 16 (2003) 63-75.

6. A.S. Pithadia, M.H. Lee, Curr. Opin. Chem. Biol. 16 (2012) 67-73.

7. L. Huang, F. Hou, J. Cheng, P. Xi, F. Chen, D. Baib, Z. Zeng, Org. Biomol. Chem. 10 (2012) 9634-9638.

8. M. Niwa, T. Hirayama, K. Okuda, H. Nagasawa, Org. Biomol. Chem. 12 (2014) 6590-6597.

9. J.P. Sumner, R. Kopelman, Analyst. 130 (2005) 528-533.

10. Y. Ma, W. Luo, P.J. Quinn, Z. Liu, R.C. Hider, J. Med. Chem. 47 (2004) 6349-6362.

11. G.E. Tumambac, C.M. Rosencrance, C. Wolf, Tetrahedron. 60 (2004) 11293-11297.

12. A. Ali, Q. Zhang, J. Dai, X. Huang, BioMetals. 16 (2003) 285-293.

13. S.M. Sethna, N.M. Shah, Chem. Rev. 36 (1945) 1-62.

14. J. Wu, R. Sheng, W. Liu, P. Wang, J. Ma, H. Zhang, X. Zhuang, Inorg. Chem. 50 (2011) 6543-6551.

15. J. Yao, W. Dou, W. Qin, W. Liu, Inorg. Chem. Comm. 12 (2009) 116-118.

16. C. Lai, B.G. Trewyn, D. Jeftinija, K. Jeftinija, S. Xu, S. Jeftinija, V.S. Lin, J. Am. Chem. Soc. 125 (2003) 4451-4459.

17. Y. Zhang, G. Wang, J. Zhang, Sens. Actuat. B: Chem. 200 (2014) 259-268.

18. R.H. Vekariya, H.D. Patel, Syn. Comm. 44 (2014) 2756-2788.

19. E.H. Kerns, L. Di, G.T. Carter, Curr. Drug Metab. 9 (2008) 879-885.

20. S. Smanmoo, W. Nasomphan, P. Tangboriboonrat, Inorg. Chem. Comm. 14 (2011) 351-354.

21. J. Nandre, S. Patil, P. Patil, S. Sahoo, C. Redshaw, P. Mahulikar, U. Patil, J. Fluoresc. 24 (2014) 1563-1570.

22. H.A. Azab, S.A. El-Korashy, Z.M. Anwar, B.H.M. Hussein, G.M. Khairy, Spectrochim. Acta A. 75 (2010) 21-27.

23. M. Mac, B. Tokarczyk, T. Uchacz, A. Danel, J. Photochem. Photobiol. A. 191 (2007) 32-41.

24. X. Poteau, A. Brown, R. G. Brown, C. Holmes, D. Matthew, Dyes Pigm. 47 (2000) 91-105.

25. M. Rauf, S. Hisaindee, J. Graham, M. Nawaz, J. Mol. Liq. 168 (2012) 102-109.

26. Y. Ma, W. Luo, P.J. Quinn, Z. Liu, R.C. Hider, J. Med. Chem. 47 (2004) 6349-6362.

27. R. Nudelman, O. Ardon, Y. Hadar, Y. Chen, J. Libman, A. Shanzer, J. Med. Chem. 41 (1998) 1671-1678.

28. L. Yang, W. Yang, D. Xu, Z. Zhang, A. Liu, Dyes Pigm. 97 (2013) 168-174.

29. J.H. Xu, Y.M. Hou, Q. Ma, X.F. Wu, X.J. Wei, Spectrochim. Acta Part A: Mol. Biomol. Spec. 112 (2013) 116-124.

30. Z.X. Li, L.F. Zhang,W.Y. Zhao, X.Y. Li, Y.K. Guo, M.M. Yu, J.X. Liu, Inorg. Chem. Comm. 14 (2011) 1656-1658.

31. V.K. Bhardwaj, A.P.S. Pannu, N. Singh, M.S. Hundal, G. Hundal, Tetrahedron. 64 (2008) 5384-5391.

32. S.I. Pascu, G. Balazs, J.C. Green, M.L.H. Green, I.C. Vei, J.E. Warren, C. Windsor, Inorg. Chim. Acta. 363 (2010) 1157-1172.

33. S. Dalapati, S. Jana, M. Alam, N. Guchhait, Sens. Actuat. B: Chem. 160 (2011) 1106-1111.

34. Y. Chiang, Y. Bhorge, R. Divate, Y. Chung, Y.J. Yen, J. Fluoresc. 26 (2016) 1699-1708.

35. Y. Chen, Y. Bhorge, A. Pape, R. Divate, Y. Chung, Y.J. Yen, J. Fluoresc. 25 (2015) 1331-1337.

36. L. Li, Z. Liu, J. Fluoresc. 27 (2016) 1-5.

37. W. He, Z. Liu, RSC Adv. 6 (2016) 59073-59080.

Graphical Abstract

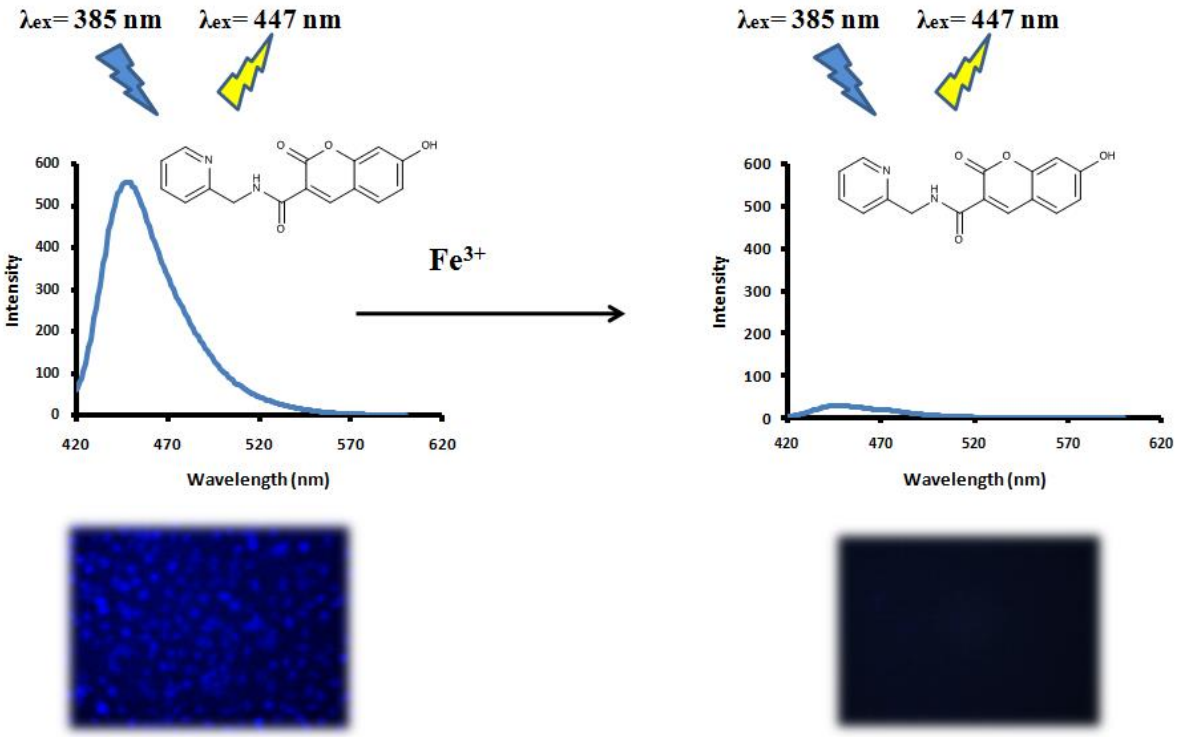

Highlights

- **Probe 1** demonstrated highly selective on-off fluorescence response in the presence of Fe^{3+} ions.
- The coumarin-based fluorescent probe exhibited 'ligand-metal charge transfer' mechanism.
- The detection limit for Fe^{3+} was found to be 0.76 μM.
- **Probe 1** can potentially be used for live cell imaging for Fe^{3+} detection.